long Wavelength Quantum Well Infrared Photodetector (QWIP) Research at Jet Propulsion Laboratory

S. 1). Gunapala, J. K. Liu, M. Sundaram, S. V. Bandara, C. A. Shott*, P. Hoelter*, P. D. Maker, and R. E. Muller

Center for Space Microelectronics Technology, Jet Propulsion Laboratory, California Institute of Technology, Pasadena, CA 91109.

* Amber, A Raytheon Company, Goleta, CA 93117.

ABSTRACT

One of the simplest device realizations of the classic particle-in-a-box problem of basic quantum mechanics is the Quantum WC]] Infrared Photodetector (QWIP). Optimization of the detector design and material growth and processing has culminated in the realization of a 1 5 μm cutoff 128x 128 focal plane array camera and a camera with large (2.56x256 pixel) focal plane array of QWIPs which can see at 8.5 μm, holding forth great promise for a variety of applications in the 6-25 μm wavelength range. This paper discusses the physics of the QWIP and QWIP technology development at Jet Propulsion Laboratory.

KEYWORDS: multi-quantum-well, intersubband, infrared detectors, long-wavelength (1 .WIR), very long wavelength (V WIR), GaAs, focal plane array, in frared camera

INTRODUCTION

Uses for infrared (IR) cameras range from the prosaic to the p rovocative. Objects at r oom temperature glow brightest in the wavelength r ange of 8 - 1 0 μm. Cameras that can see 8-10 μm lig ht find uses in security and surveillance, navigation and flight co ntrol, early-warning systems, etc. Such a camera's ability to produce a thermal map of the surface of human skin offers applications in medical imaging. Since most of the absorption lines of gas molecules lie in the long wavelength in frared (1 .WIR) spectral region, IR ca meras can be used to monitor and measu re pollution, relative humidity profiles, and the distribution 01 di fferent gases in the atmosphere. The absorption li ne s of many gas m olec ules , such as ozone, water, carbon monoxide, carbon dioxide, and nitrous oxide occur in the wavelength region from 3 to 18 μm. Thus, IR imaging systems that operate in the very long wavelength IR (VWIR) region (12 - 18 μm) are also required in many space applications such as monitoring the global atmospheric temperature profiles, relative humidity profiles, cloud characteristics, and the distribu tion of minor constituents in the atmosphere which are being pla nne d for NASA's Earth Observing System [1]. Ground- based telescopes fitted with these cameras can stare out the 8-12 μm tra n sparent window in the earth's atmosphere, i m a g e distant stars and galaxies (including those invisible to telescopes equipped with normal visible cameras), and help in the search for cold objects such as planets orbiting nearby stars.

Science, defense, and commerce all stand to benefit from sharper, affordable IR cameras. Recent developments at the Jet Propulsion Laboratory have culminated in very sensitive yet affordable LWIR and VWIR cameras.

THE QWIP

A quantum well designed thus to detect infrared light is called a Quantum Well Infrared Photodetector (QWIP). An elegant candidate for QWIP is the square. quantum well of basic quantum mechanics. When the quantum well is sufficiently deep anti narrow, its energy slates are quantized (discrete). The potential depth and width of the well can be adjusted so that it holds only two energy states: a ground state near the well bottom, and a first excited state near the well top. A photon striking the well will excite an electron in the ground state to tile first excited state, whence an externally-applied voltage sweeps it out producing a photocurrent (Fig. 1). only photons having energies corresponding to the energy separation between the two states arc absorbed, resulting in a detector with a sharp absorption spectrum. Designing a quantum well to detect light of a particular wavelength becomes a simple matter of tailoring the potential depth and width of the well to produce two states separated by the desired photon energy.

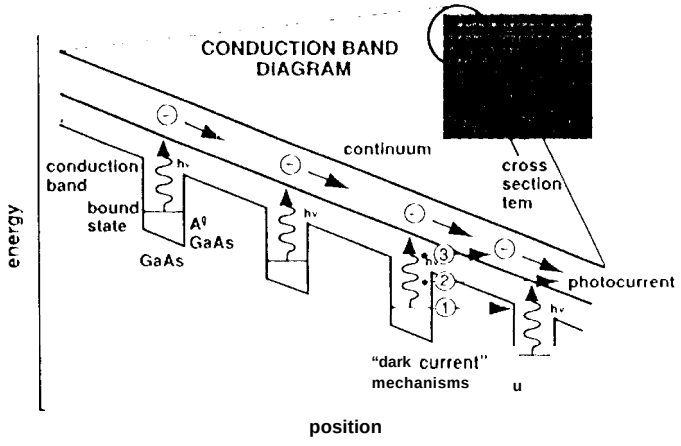

Fig. 1 Schematic diagram of the conduction band in a bound-to-continuum QWIP in an externally applied electric field. Absorption of IR photons can photoexcite electrons from the ground state of the quantum well into the continuum, causing a photocurrent. Three dark current mechanisms are also shown: ground state tunneling (1); thermally assisted tunneling (2); and thermionic emission (3).

The QWIP might have remained a textbook curiosity had it not been for the spectacular advances within the last 20 years in the crystal growth and processing techniques of large bandgap compound semiconductors such as GaAs and $Al_xGa_{1-x}As$. A quantum well can be realized by sandwiching a layer of GaAs between two layers of $Al_xGa_{1-x}As$. The well width is controlled by controll ing the GaAs layer thickness; the potential depth is controlled by controlling the Al composition x in the barrier layers. Modern crystal-growth methods like molecular beam epitaxy (MBE) allow the growth of highly uniform and pure crystal layers of such semiconductors on large substrate wafers, with control of cacti layer thickness down to a fraction of a molecular layer. In other words, a textbook square quantum well Of the desired shape can be produced. The $GaAs/Al_xGa_{1-x}As$ material system allows tile quantum well shape to be tweaked over a range wide enough to enable light detection at wavelengths longer than ~6 μm. Stacking several identical quantum wells (typically 50) together increases photon absorption. Ground state electrons arc provided in the detector by doping the GaAs well layers with Si. Fabricated entirely from large bandgap materials which arc easy to grow and process, it is now possible to obtain large uniform FPAs of QWIPs tuned to detect light at wavelengths longer than ~6 μm in the $GaAs/Al_xGa_{1-x}As$ material system.

DARK CURRENT

Improving QWIP performance depends largely on minimizing the parasitic current that plagues all light detectors: the dark current (the current that flows through a biased detector in the dark, i.e., with no photons

impinging on it). The dark current in QWIPs originates from three different mechanisms (Fig. 1). Sequential tunneling of ground state electrons from well to wc]] dominates the dark current at temperatures less than 30 K and can bc reduced by widening the barriers. At intermediate temperatures, a second mechanism kicks in: thermionic emission of ground state electrons toward the well top followed by tunneling through tile barrier tip in(o the energy continuum above the wells and barriers. At temperatures above 45 K, the dark current is entirely dominated by classic thermionic emission of ground slate. electrons directly out of the well into the energy continuum. Minimizing this last component is critical to the commercial success of the QWIP as it allows the highly-desirable high-temperature camera operation.

Wc design the ***bound-to-quasibound*** quantum wcli by placing the first excited state exactly at the well top (Fig. 2,). The best previous QWIPs (pioneered by Barry Levine *et al.* [2] at AT&T Bell Labs) were of the bound-to-continuum variety, so-called because the first excited state was a continuum energy band above the well top (typically 10-15 meV). Dropping the. first excited state to the wc1l top causes the barrier to thermionic emission (roughly the energy height from the. ground state to the well top) to bc - 15 meV nmrc in our bound-to-quasibound QWIP than in the bound-to-continuum one, theoretically causing the dark current 10 drop by a factor of -20 at a temperature of 70 K. This compares well with the factor of - 12 drop wc experimentally observe (Fig. 2). importantly, the bound-to-quasibound QWIP still preserves the photocurrent. Onc could push the first excited state deeper into the well to increase the barrier to thermionic emission even fill ther, but this would drop the photocurrent to unacceptably low levels.

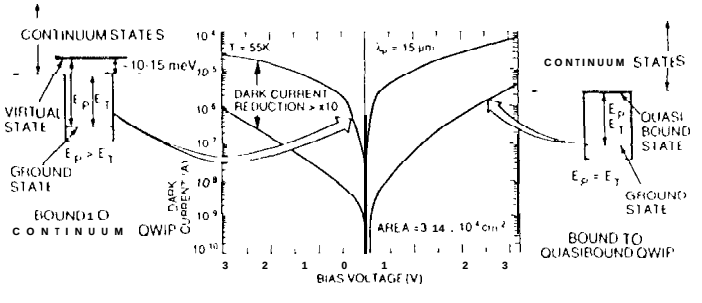

Fig. 2 Comparison of dark currents of bound-to-continuum and bound-to-quasicontinuum VWIR QWIPs as a function of bias voltage at temperature T = 55 h'.

Wc further reduce the dark current by drastically cutting the well doping density to decrease the number of ground state electrons available for thermionic emission, and by increasing each barrier thickness in the multi-quantum-well (MQW) stack to 60 nm; any further decrease in well doping or increase in barrier thickness causes no significant enhance in signal-to-noise ratio.

LIGHT COUPLING

A key factor in QWIP focal plane array (FPA) performance is the light coupling scheme. This is caused by a selection rule peculiar to GaAs/Al$_x$Ga$_{1-x}$As QWIPs: light striking the quantum well layers normally is *not* absorbed; to bc absorbed, the light has to have a component of its electric field in the quantum well direction [3]. Light being a transverse wave, this requires bending the normally incident light inside tile detector-. This is done with mirrors.

A simple scheme is to put a special mirror on the detector top and illuminate the detector from the back. A *smooth* top mirror is useless: it simply reflects the light straight back out. '1'0 bc useful, the mirror has to bc *rough* (on the scale of the light's wavelength in GaAs). 1 ight normally entering through the back side anti striking a rough top mirror is scattered back in a cone. This cone now strikes the back side. '1'hose rays that arc within a critical angle of the normal (] '/° for the GaAs-air IntcI'face) escape out. The rest suffer tots] internal reflection with the back surface acting as a smooth mirror. The internally reflected rays are once again reflected

off the top rough mirror. What happens next depends on whether the roughness of the top mirror is pet-iodic or random. If it is periodic, the top mirror will bend these rays so that they are all normal to the quantum well layers again. These rays pass through the detector and out from the back side. A *randomly* roughened mirror, on the other hand, will randomly scatter all the rays internally reflected on to it from the back side *each time*, allowing the incident light to bounce back and forth between the detector top and back surfaces several times (Fig. 3). Only light within a 1-7° (from normal) cone escapes out from the back side. Clever design can reduce the amount of light in the escape cone but cannot eliminate it altogether. For instance, if the random reflector is designed with two levels of rough surfaces having the same areas but located a quarter wavelength apart, the *normally* reflected light intensities from the top and bottom surface.s of the reflector arc equal and 180° out of phase (i.e., phase plate). This maximizes the destructive interference at normal reflection and lowers light leakage through the escape cone [3].

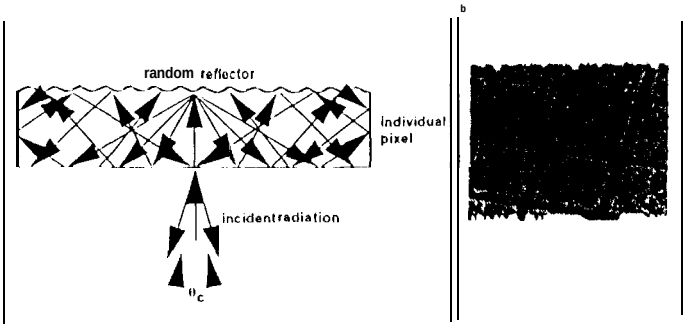

Fig. 3 (a) Schematic side view of a thin QWIP pixel with a random reflector. Ideally all the radiation is trapped except for a small fraction which escape through the escape cone (defined by critical angle Qc), (b) Random reflectors on pixels in a focal plane array.

On each pass through the MQW region some of the bent light is absorbed. A periodic mirror thus offers two useful passes, a random mirror several. Trapping the most light with a rough mirror requires increasing the detector aspect ratio (diameter/height), accomplished by thinning the - 600 μm thick GaAs substrate on top of which the MQW stack is grown, to about zero. This approximately *doubles* the light absorbed in the periodic mirror case; it *quadruples* it when a random mirror is used.

15 μm CUTOFF 128X128 FOCAL PLANE ARRAY CAMERA

The device structure consists of 50 periods containing 6.5 nm wells of GaAs (doped $n = 2x10^{17} cm^{-3}$) and 600 Å barriers of $Al_{0.15}Ga_{0.85}As$ (sandwiched between 0.5 μm GaAs top and bottom contact layers doped $n = 2.x\ 1\ 0^{17} cm^{-3}$) grown on a semi-insulating GaAs substrate by molecular beam epitaxy (MBE). Then a 1.1 μm thick GaAs cap layer On top of 30 nm $Al_{0.15}Ga_{0.85}As$ stop-etch layer was grown *in situ* on top of the device structure to fabricate the light coupling optical cavity, The MBE grown QWIP structure was processed into 2,00 μm diameter mesa test structures (area $= 3.14 \times 10^{-4} cm^2$) using wet chemical etching, and Au/Ge ohmic contacts were evaporated onto the top and bottom contact layers. The dark current-voltage curves of the QWIP was measured as a function of temperature from '1' = 30-60 K and the T = 55 K curve is shown in Fig. 2.

The responsivity spectra of these detectors were measured using a 1000 K blackbody source and a gratin: monochromator. The absolute peak responsivities (R_p) of the detectors were measured using a calibrated blackbody source. The detector were back illuminated through a 45° polished facet [3] and its responsivity spectrum is shown in Fig. 4. The responsivity of the detector peak at 14.2 μm and the peak responsivity (R_p) of the detector is 420 mA/W. The spectral width and the cutoff wavelength are $\Delta\lambda/\lambda = 13\%$ and $\lambda_c = 14.9$ μm. The bias dependent peak responsivity of the detector is shown in Fig. 4. The measured absolute responsivity of the detector is small up to about $V_B = 1$ V. Beyond that it increases nearly linearly with the bias reaching RP = 560 n IA/W at $V_B = 4$ V. This type of behavior of responsivity versus bias is typical for a bound-to-quasibound QWIP. The peak quantum efficiency was 3% (lower quantum efficiency is due to the lower we]] doping density) for a 45" double pass.

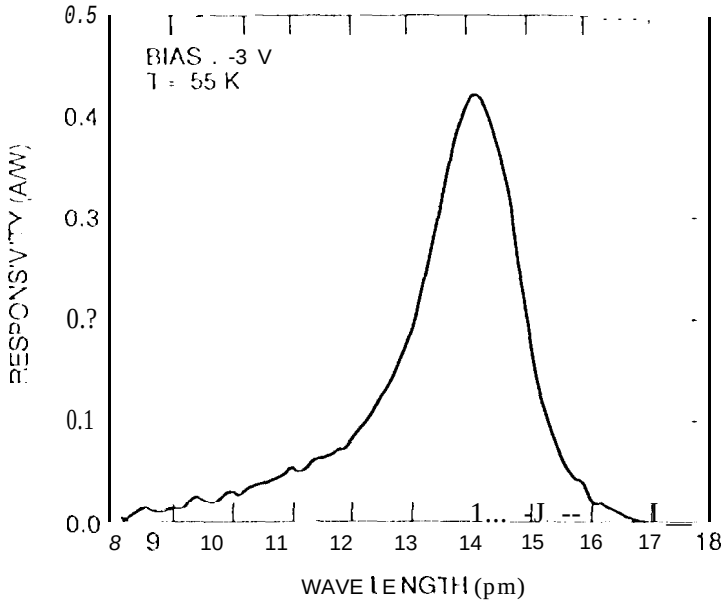

Fig. 4 Responsivity spectra of a bound-to-quasicontinuum VWIR QWIP focal plane array sample at temperature T = 55 K. The spectral response peak at 14.2 μm and the long wavelength cutoff is at 14.9 μm.

The current noise in was measured using a spectrum analyzer and experimentally determined the photoconductive gain g using $g = i_n^2 / 4eI_D B$ - t 1/2N, where B is the measurement band width and N is the number of quantum wells. Photoconductive gain of the detector reached 0.32 at V_B = -6 V. Since the gain of QWIP is inversely proportional to tile number Of quantum wells **N,** the better comparison would be the well capture probability p_c, which is directly related to the gain by $g = 1/Np_c$. The calculated well capture probabilities are 20% at low bias and 6% at high bias voltage which indicate the excellent hot-electron transport in this device structure. The peak detectivity is defined as $D_p^* = R_p \sqrt{AB} / i_n$, where RP is the peak responsivity, A is the area of the detector and A = 3.14x1 ()'1 cm^2. The measured peak detectivity at bias V_B = -3 V and temperature T = 55 K is $1.6x10^{10}$ cm/√11z/W.

The photoconductive QWIPs of the 128x128 FPAs were then fabricated by wet chemical etching through the photosensitive GaAs/$Al_xGa_{1-x}As$ multi quantum well layers into the 0.5 μm thick doped GaAs contact layer. The pitch of the. FPA is 50 μm and the actual pixel size is 38x38 μm^2. Then the random reflectors on the top of the detectors were covered with Au/Ge and Au for Ohmic contact and reflection. Then indium bumps were evaporated on top of the detectors for Si read out circuit (ROC) hybridization. A single QWIP FPA was chosen (cutoff wavelength of this sample is 14.9 μm) and bonded to a 128xl'28 Si multiplexer (Amber AE- 159) and biased at V_b = -2.7 V. The FPA was back-illuminated through the flat thinned substrate (thickness 25 μm). This initial array gave excellent images with 99.9% of the pixels working, demonstrating the high yield of GaAs technology. Figure 5 clearly shows the excellent uncorrected photocurrent uniformity (pixel-to-pixel) of the 16384 pixels of the 128x128 FPA with a standard deviation of only = 2.4%. The uniformity after correction was 0.2%. As mentioned earlier this high yield is due to the excellent GaAs growth uniformity and the mature GaAs processing technology.

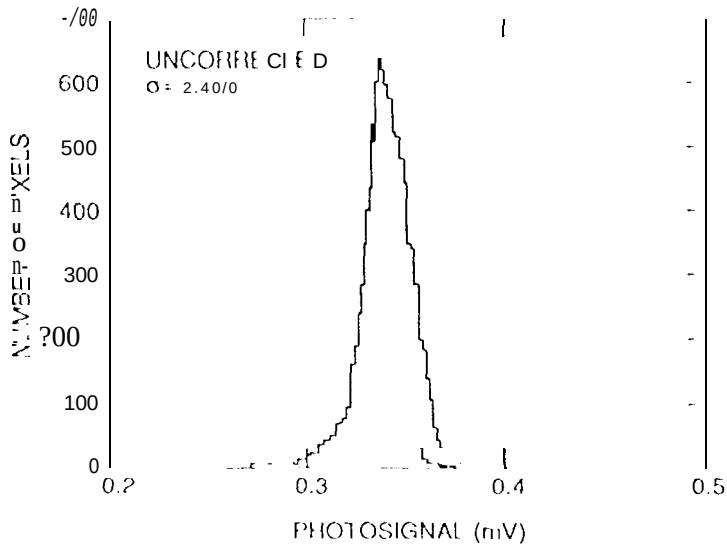

Fig. 5 Photosignal histogram of the 16384 pixel of the 128x128 array showing a high uniform uncorrected standard deviation of only = 2.4%.

Video images were taken at various frame rates varying from 50 to 200 1 Iz with f/2.3 KRS-5 optics at temperatures as high as T = 45 K, using a ROC capacitor having a charge capacity of $4x10^7$ electrons. Figure 6 shows an image of a man's face taken with a QWIP FPA camera. The measured noise equivalent temperature difference N}{A'I' of the FPA was 30 mK at an operating temperature of T = 45 K for 300 K background. This reasonably agrees with our calculated value of 10 mK. We have used the following equation to calculate the NEAT of the FPA.

$$NEAT = \frac{\sqrt{AB}}{D_B^*(dP_B / dT)\sin^2(\theta / 2)} \quad (1)$$

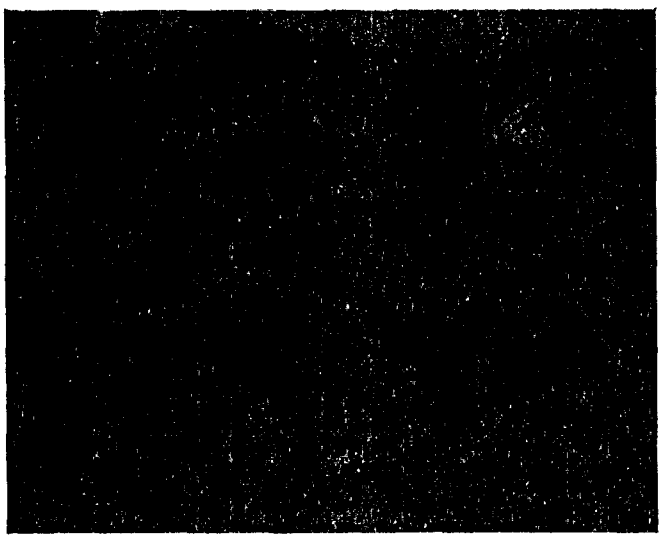

Fig. 6 One frame from a 15 μm QWIP video image of a man's face with NEAT = 30 mK. The warm air from his nostrils can be clearly seen.

where D_B^* is the blackbody detectivity, dP_B / dT is the derivative of the integrated blackbody power with respect to temperature, and is the field of view angle [i.e., $\sin^2(\theta/2) = (4f^2+1)^{-1}$, where f is the f number of the optical system]. No band pass filters were. used and are unnecessary in QWIP camera systems because of the narrow spectral response of QWIPs. It should be noted that these initial unoptimized FPA results are far from optimum. The QWIP cic.vice structures was not optimized; the gratings were also not optimized for the maximum light coupling efficiency; no micro lenses were used; no antireflection coatings were used; the substrate was not thinned enough (the hybrid was thinned to 25 μm, however, it was not sufficient to improve the. light coupling efficiency to small pixel and in fact this explains the slightly higher measured NEAT); and finally the multiplexer used was a photovoltaic InSb multiplexer which is certainly not optimized to supply the proper bias and impedance levels required by photoconductive QWIPs. Implementation of these improvements should significantly enhance the QWIP focal plane array operating temperatures (i.e., 55 K for 15 μm).

9 μm CUTOFF 256X256 I I AN])-] IELD CAMERA

The QWIP device structure consists of 50 periods, each period containing a 511111 well of GaAs (doped n $4x10^{17}$ cm-3) and a 60 nm barrier of $Al_{0.3}Ga_{0.7}As$, sandwiched between 0.5 μm GaAs top and bottom contact layers doped $11 = 5x10^{17}$ cm^{-3}, grown on a semi-insulating GaAs substrate by molecular beam epitaxy (MBE). Then a 0.7 μm thick GaAs cap layer on top of a 30 nm Al. $_3Ga_{0.7}As$ stoj)-etch layer was grown *in situ* on *top* of the device structure to fabricate the light coupling, optical cavity. The MBE grown QWIP structure was processed into 200 μm diameter mesa test structures as described earlier. Theoretically this bound-to-quasibound QWIP should give a factor of 3 lower dark current than bound-to-continuum QWIP (with first excited state placed 6 meV above the barrier threshold) and it closely agrees with the experimental value of a f-actor of 4 higher dark current at bias $V_B = -2V$.

The responsivity spectra of these detectors were measured using a i 000 K blackbody source and a grating monochromator. The absol ute peak responsivities (R_p) of the detectors were measured using a cal ibrated

blackbody source. The detectors were back illuminated through a 45° polished facet [3] and a responsivity spectrum is shown in Fig. 7. The responsivity of the detector peaks at 8.5 μm and the peak responsivity (R_p) 01 the detector is 300 mA/W at bias V_B = -3 V. The spectral width and the cutoff wavelength are $\Delta\lambda / \lambda$ = 10% and λ_c = 8.9 μm respectively. The measured absolute peak responsivity of the detector is small up to about V_B = -0.5 V. Beyond that it increases nearly linearly with bias reaching R_P = 380 m A/W at V_B = -5 V. This type of behavior of responsivity versus bias is typical for a bound-to-q uasibound QWIP. The peak quantum efficiency was 6.9% at bias V_B = -1 v (lower quantum efficiency is due to the lower well doping density) for a 45° double pass. The current noise in was experimentally n ieasured and the photoconductive gain g was determined as described earlier. The photoconductive gain Of the detector reached 0.98 at V_B = -5 V. The calculated well capture probabilities are 25% at low bias (i.e., V_B = -1 V) and 2% at high bias (i.e., V_B = -5 V) which together indicate the excellent tlot-electron transport in this device structure. The peak detectivity is defined as $D^*_p = R_p \sqrt{AB} / i_n$, where R_P is the peak responsivity, A is the area of the detec tor and A = 3.14×10^{-4} cm^2. The measured peak detectivity at bias V_B = -3. ? V and temperature T = 70 K is 2.3×10^{11} cm√Hz/W. These detectors show background limited performance (BLIP) at bias V_B = -? V and temperature T = 72 K for 300 K background with f/2 optics

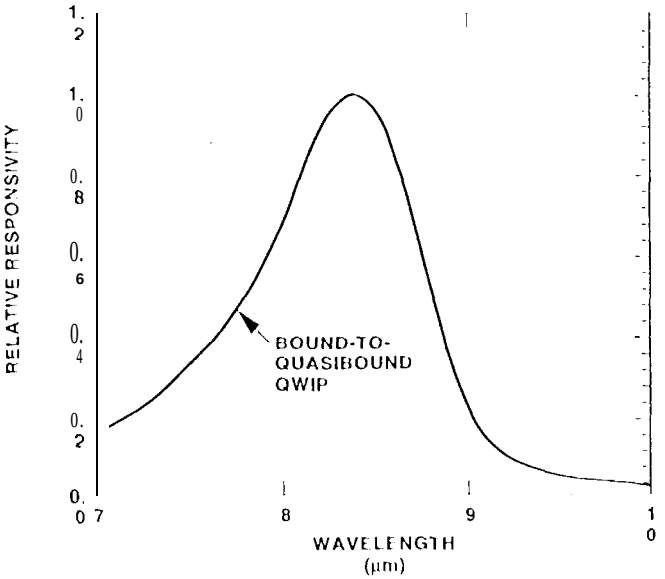

Fig. 7 Responsivity spectrum of a bound-to-quasibound LWIR QWIP test structure at temperature T = 77 K. The spectral response peak is at 8.5 μm and the long wavelength cutoff is at 8.9 μm.

The QWIP imagin g arrays were fabricated as described earlier. The pitch of the FPA is 38 μm; the actual pixel size is 28 μm x 28 pm. Figure 8 shows a picture of twclIty-five 2.56x256 pixel QWIP FPAs on a 3-inch GaAs wafer-, produced by the Jet I'repulsion laboratory. Indium bumps were then evaporated on the tops of the detectors for Si readout circuit (ROC) hybridization. A single QWIP FPA was chose.n and hybridized or mated (via an indium bump-bonding process) to a matching 256x256 pixel CMOS multiplexer (Amber AE-166), and biased at V_B = - 1 V.

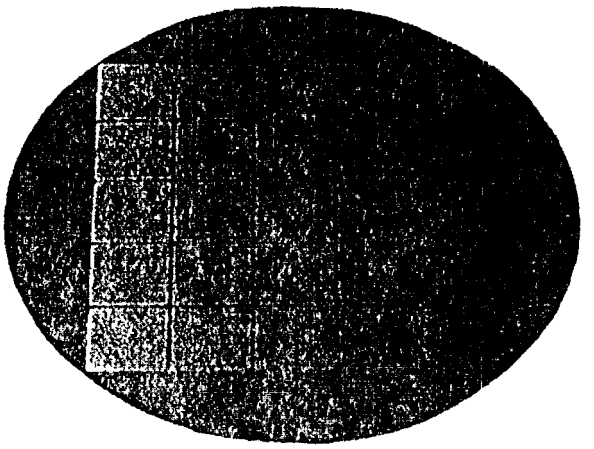

Fig. 8. Twenty five 256x256 QWIP focal plane arrays on a 3 in. GaAs wafer.

At temperatures below 72 K, the signal-to-noise ratio of the system is limited by array non-uniformity, multiplexer readout noise, and photo current (photon flux) noise. At temperatures above 72 K, temporal noi se due to the QWIP's higher dark current becomes the limitation. The FPA was back-illuminated through the flat thinned substrate membrane (thickness 130 nm). The measured mean NEAT of the FPA with 110 lens was 26 mK at an operating temperature of '1' = 70 K and bias V_B = -1 V, for a 300 K background. This initial array gave excellent images with 99.98% of the pixels working (number of dead pixels 10), demonstrating the high yield of GaAs technology.

A 256x256 QWIP FPA hybrid was mounted on to a 450 mW integral Sterling closed-cycle cooler assembly and installed into an Amber RADIANCE[1M] camera-body, to demonstrate a hand-held 1 .WIR camera (shown in Fig. 9). The camera is equipped with a 32-bit floating-point digital signal processor combined with multi-tasking software, providing the speed and power to execute complex image-processing and analysis functions inside the camera body itself. The other element of the camera is a 100 mm focal length germanium lens, with a **5.5** degree field of view, It is designed to be transparent in the 8-12 μm wavelength range, to be compatible with the Q WIP's 8.5 μm operation. The digital acquisition resolution of the camera is 12-bits. Its nominal power consumption is less than 50 Watts.

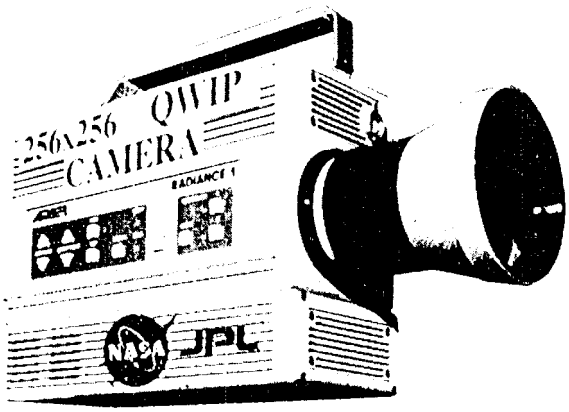

Fig. 9 Picture of the first 256x256 hand-held long wavelength QWIP camera (QWIP RADIANCE).

The measured mean NEAT of the QWIP camera is 40 mK (the higher NEAT is due to the lens assembly cutting the light transmission by **35%)** at an operating temperature of 'i' = 70 K and bias V_B = -1.5 V, for a 300 K background. The peak quantum efficiency of the FPA is 3%, corresponding to an average of 3 passes of] R radiation through the photosensitive multi-quantum well region. The low quantum efficiency can be partly attributed to the fact that the substrate reflects 30% of the light striking it; and the fact that the array has a 65% fill factor, i.e., the detectors cover oniy 65% of the array surface, with the remaining 35% being the dead space between detectors. The uncorrected photocurrent non-uniformity (which includes a 1% non-uniformity of the ROC and a 1 .4% non-uniformity due 10 the cold-stop in front of the FPA not yielding the same field of view to all the pixels) of the 65,536 pixels of the. '256x256 FPA is about 6.8% (= sigma/mean). The non-uniformity after two-point (1 '/° and 27° Celsius) correction improves to an impressive 0.05%. As mentioned earlier, this high yield is due to the excellent GaAs growth uniformity and the mature GaAs processing technology.

Video images were taken at a frame rate of 601 Hz at temperatures as high as "1' = 70 K, using a ROC capacitor having a charge capacity of 9×10^6 electrons (the maximum number of photoelectrons and dark electrons that can be counted in the time taken to read each detector pixel). Figure 10 (a) shows one frame of a video

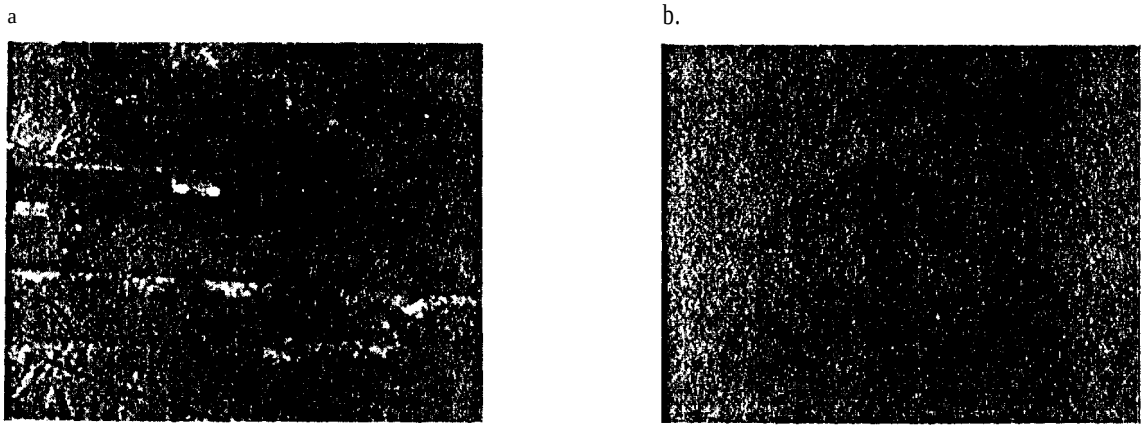

Fig. 10 (a) Shows one frame of a video image taken with a 9 μm cutoff 256x256 QWIP camera at night The van shown in the picture was about one mile away from the camera. (b) An absorption image of acetone fumes (acetone has a strong IR absorption at 8.8 μm) taken with the same camera.

image taken with a 9 μm cutoff 256x256 QWIP camera at night. The van shown in the picture was about one mile away from the camera. Figure 10(b) shows an absorption image of acetone fumes (acetone has a strong IR absorption at 8.8 μm) taken with the same camera. These images demonstrate the high sensitivity of the 256x256 QWIP staring array camera.

SUMMARY

Exceptionally rapid progress has been made in the development of long wavelength QWIPs, since they were first experimentally demonstrated several years ago. It is now possible for QWIPs to achieve excellent performance (e.g., detectivities as high as D* - Ix 10^{11} cm√Hz/W at 70 K for a 9 μm QWIP) and be fabricated into large inexpensive low-noise imaging arrays. A 70 K operating temperature can be easily achieved by sill~lc-stage Stirling cycle coolers, which allows us to demonstrate the first han(l-held 256x256 FPA LWIR camera based on QWIPs. Weighing about ten pounds, the QWIP RADIANCE I camera is entirely self-contained, with no extra boxes for control, cooling, or image processing. Its sharp, inexpensive, large, uniform, infrared eye (which can be tailored to see a particular IR wavelength) makes the QWIP hand-held camera the best and the most cost-effective new tool for imaging and spectroscopy in the interesting 8-14 μm wavelength 1 ange.

ACKNOWLEDGMENTS

The research described in this paper was performed by the Center for Space Microelectronics Technology, Jet Propulsion Laboratory, California Institute Of Technology, and was jointly sponsored by the BMDO/IS&T office, and the NASA Office of Space Access and Technology.

REFERENCES

[1] M. '1'. Chahine, "Sensor requirements for Earth and Planetary Observations," Proceedings of Innovative Long Wavelength Infrared Detector Workshop, Pasadena, California, pp. 3-3 i , April ?4-26, 1990.

[2] B. II'. Levine, C. G. Bethea, G. Hasnain, V. O. Shen, E. Pelve, R. R. Abbott, and S. J. Hsieh, "High sensitivity low dark current 10 μm GaAs quantum well infrared photodetectors," Appl. Phys. I cit., vol. 56, pp. **851-853,** 1990.

[3] S. 1). Gunapala and K. h4. S. V. Bandara, Physics of Thin J ilms, Academic Press, 2 i , 113 (1995), and references therein.